

# Temperature Sensitive Nanocapsule of Complex Structural Form for Methane Storage

E. I. Volkova · M. V. Suyetin · A. V. Vakhrushev

Received: 11 September 2009 / Accepted: 5 October 2009 / Published online: 16 October 2009  
© to the authors 2009

**Abstract** The processes of methane adsorption, storage and desorption by the nanocapsule are investigated with molecular-dynamic modeling method. The specific nanocapsule shape defines its functioning uniqueness: methane is adsorbed under 40 MPa and at normal temperature with further blocking of methane molecules the  $K@C_{60}^{1+}$  endohedral complex in the nanocapsule by external electric field, the storage is performed under normal external conditions, and methane desorption is performed at 350 K. The methane content in the nanocapsule during storage reaches 11.09 mass%. The nanocapsule consists of three parts: storage chamber, junction and blocking chamber. The storage chamber comprises the nanotube (20,20). The blocking chamber is a short nanotube (20,20) with three holes. The junction consists of the nanotube (10,10) and nanotube (8,8); moreover, the nanotube (8,8) is connected with the storage chamber and nanotube (10,10) with the blocking chamber. The blocking chamber is opened and closed by the transfer of the  $K@C_{60}^{1+}$  endohedral complex under electrostatic field action.

**Keywords** Methane storage · Nanocapsule · Molecular dynamics

## Introduction

The bucky shuttle [1, 2] being the combination of nanosize carbon structures—fullerene [3] and nanotube [4], has many possible applications: nanoscale storage cells [5], devices for directed medicine transfer [6] and containers for effective and safe gas storage [7–13]. Nanosize containers and capsules of various shapes that allow reaching a higher safety level and mass content of gas stored have been investigated for a number of years [11–13]. The engineering of nanostructured carbon opens the ways for the production of nanocapsules of complex structural shapes [14–16].

In this work, the processes of methane molecule adsorption, storage and desorption by the nanocapsule are investigated with molecular-dynamic modeling method. The nanocapsule-specific structure defines its adsorption qualities: at the storage stage under normal conditions, the nanocapsule contains the amount of methane that was adsorbed at normal temperature and under 40 MPa. Methane is stored in the nanocapsule under normal external conditions. The nanocapsule desorption takes place at the temperature elevation up to 350 K. There is no need to apply electric field during storage and desorption.

## Computational Model and Details

Methane adsorption, storage and desorption processes were modeled with the method of molecular dynamics. The calculations were made with the program NAMD [17] in force field CHARMM27. The calculation results obtained were visualized with the program VMD [18]. The values of hydrogen and carbon atom charges in methane molecule were obtained [11] using the combination of Hartree–Fock

E. I. Volkova  
Izhevsk State Technical University, Studencheskaya str., 7,  
426069 Izhevsk, Russia

M. V. Suyetin (✉) · A. V. Vakhrushev  
Institute of Applied Mechanics UB RAS, T.Baramzinoy str., 34,  
426067 Izhevsk, Russia  
e-mail: msuyetin@gmail.com

and Becke exchange with Lee–Yang–Parr correlation potential: B3LYP/6-31G(d) [19, 20]. The calculations were made with the program Gaussian [21]. The following atom charge values in methane molecule were obtained: carbon atom  $-0.628204$  Mulliken and hydrogen atom  $+0.157051$  Mulliken.

The object of investigation is the nanocapsule whose structure is demonstrated in Fig. 1.

The nanocapsule consists of three parts: storage chamber, junction and blocking chamber. The storage chamber comprises the nanotube (20,20). The blocking chamber is a short nanotube (20,20) with three holes. The junction consists of the nanotube (10,10) and nanotube (8,8), moreover, the nanotube (8,8) is connected with the storage chamber, and nanotube (10,10) with the blocking chamber. The blocking chamber is opened and closed by the transfer of the  $\text{K@C}_{60}^{1+}$  endohedral complex under electrostatic field action. The charge of  $+1|e|$  of the  $\text{K@C}_{60}^{1+}$  endohedral complex is uniformly distributed over the  $\text{C}_{60}$  shell. The nanotube (8,8) in the junction prevents the  $\text{K@C}_{60}^{1+}$  from entering the storage chamber. The nanotube (8,8) diameter is rather large for the penetration of methane molecules, but small for the transition of the  $\text{K@C}_{60}^{1+}$ . Each hole in the blocking chamber is formed as a result of removing 24 carbon atoms. Dangling bonds are saturated by hydrogen atoms. The holes obtained are large enough for free penetration of methane molecules into the nanotube internal space. The experiment on obtaining similar holes with the application of electron beams is described in [14]. It is shown that the beams can be focused on the area  $1 \text{ \AA}$  in diameter. The holes in the nanotube can exist at the temperatures up to  $400 \text{ K}$ ; when the temperature elevates, the hole diameter in the nanotubes considerably decreases due to the motion and fusion of single vacancies [8–10]. During modeling, it is imitated that the nanocapsule is

placed on the substrate, i.e., the nanotube base is fixed—the nanocapsule left end is demonstrated in Fig. 1. The change in the nanotube diameter is also possible with the methods of nanostructural engineering [14].

The charged endohedral complex  $\text{K@C}_{60}^{1+}$  moves in the blocking chamber and junction under the action of external electric field. The electric field direction defines the nanocapsule state in the operation cycle: methane adsorption, its storage and desorption. The value of external electric field intensity, required for the  $\text{K@C}_{60}^{1+}$  to move, equals  $3.045 \times 10^9 \text{ V/m}$ . The motion of charged fullerene in the nanotube with the help of electric field is described in detail in [5].

## Results and Discussion

The nanocapsule operation can be split into several stages: methane adsorption, storage and desorption.

At the adsorption stage (Fig. 2), the  $\text{K@C}_{60}^{1+}$  endohedral complex is retained at the end of the blocking chamber under the action of Van der Waals forces. The methane molecules from the environment freely penetrate through the three holes into the blocking chamber and adsorb into the external space of the storage chamber. The external thermodynamic conditions are  $T = 300 \text{ K}$  and  $P = 40 \text{ MPa}$ . The storage chamber space adsorbs 485 methane molecules, which is 11.09 mass%.

The calculations are based on the following formula (1):

$$\text{mass} = \frac{N_{\text{CH}_4} \times m_{\text{CH}_4}}{N_{\text{CH}_4} \times m_{\text{CH}_4} + N_{\text{C}} \times m_{\text{C}}} \times 100\% \quad (1)$$

where  $N_{\text{CH}_4}$ —number of methane molecules,  $N_{\text{C}}$ —number of carbon atoms in the nanotube,  $m_{\text{CH}_4}$ —mass of one methane molecule and  $m_{\text{C}}$ —mass of one carbon atom.

**Fig. 1** Nanocapsule for natural gas storage, consisting of storage chamber, junction and blocking chamber

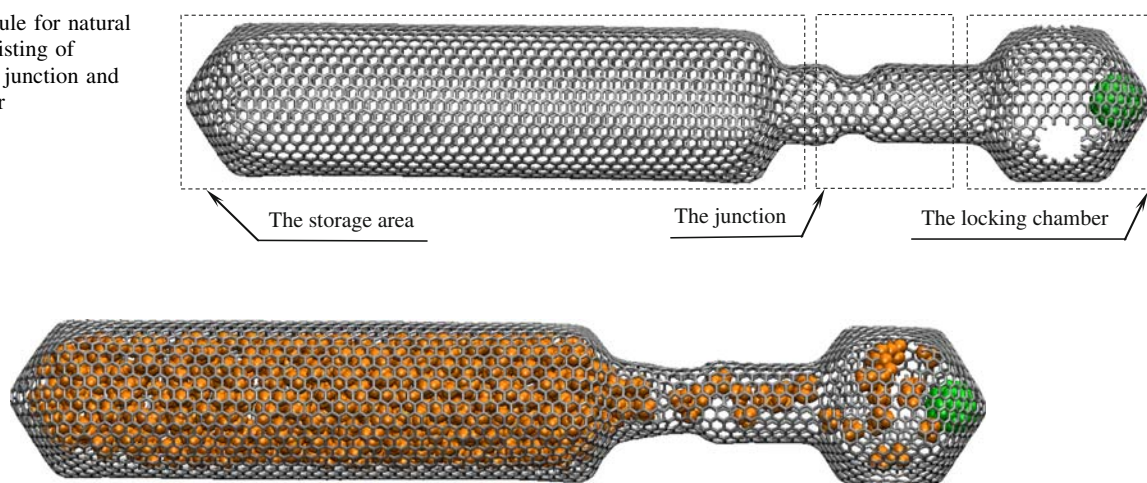


**Fig. 2** Adsorption stage ( $T = 300 \text{ K}$ ,  $P = 40 \text{ MPa}$ )

Figure 3 demonstrates the nanocapsule filling dynamics with methane at 300 K and under 40 MPa. It is clearly seen that 4 ps is enough to complete the filling of the nanocapsule storage area.

To block methane molecules in the storage chamber, it is necessary to move the  $\text{K@C}_{60}^{1+}$  ion into the junction with the help of electric field as shown in Fig. 4. External thermodynamic conditions are  $T = 300$  K and  $P = 40$  MPa. Further motion of the  $\text{K@C}_{60}^{1+}$  is blocked by the junction narrow part—nanotube (8,8).

Figure 5 demonstrates the dependencies of the change in the  $\text{K@C}_{60}^{1+}$  position and its kinetic energy under the electric field action in the blocking chamber upon time. A sharp increase in the  $\text{K@C}_{60}^{1+}$  kinetic energy equaled to 0.254 eV is observed at 0.5 ps, at the same time the velocity reaches 327 m/s. This is explained by the electric field action on the  $\text{K@C}_{60}^{1+}$ . At  $t = 1$  ps, the  $\text{K@C}_{60}^{1+}$  kinetic energy decreases significantly, reaching 0.000255 eV and further up to 15 ps its value does not considerably increase. This is explained by minor oscillations of the  $\text{K@C}_{60}^{1+}$  near the right end of the blocking chamber. The  $\text{K@C}_{60}^{1+}$  is retained due to Van der Waals forces. Under the constant action of electric field, the  $\text{K@C}_{60}^{1+}$  kinetic energy increases again and reaches 0.61 eV at  $t = 16.5$  ps, i.e., the  $\text{K@C}_{60}^{1+}$  breaks off the blocking chamber and moves to the storage chamber to block its entrance.

In the time period from  $t = 16.5$  ps to  $t = 26.5$  ps, the considerable attenuating oscillations of the kinetic energy conditioned by the  $\text{K@C}_{60}^{1+}$  motion along the blocking chamber walls adjacent to the junction entrance are observed. In this time period, each peak of the  $\text{K@C}_{60}^{1+}$  kinetic energy corresponds to the time moments after passing the pentagonal rings in the structure of the blocking chamber. Under the electric field action, the  $\text{K@C}_{60}^{1+}$  penetrates into the right end of the junction—nanotube (10,10)—and blocks the outlet of methane molecules from the storage chamber. During the penetration, a considerable increase in the kinetic energy is observed, its maximum value reaches 0.63 eV at  $t = 32$  ps. After the  $\text{K@C}_{60}^{1+}$  passes the nanotube (10,10), the kinetic energy sharply decreases conditioned by the  $\text{K@C}_{60}^{1+}$  deceleration in the portion of the nanotube (8,8). In the interval from  $t = 41.5$  ps to  $t = 48.5$  ps, the insignificant fluctuations of the  $\text{K@C}_{60}^{1+}$  position connected with the compressed gas pressure from one side and electric field action from another are observed. The value of the  $\text{K@C}_{60}^{1+}$  kinetic energy does not exceed 0.033 eV. In the process of methane molecules adsorption, the maximum velocity of the  $\text{K@C}_{60}^{1+}$  motion is 515.5 m/s ( $t = 32$  ps).

When transferring to the storage stage, the electric field switches off, and external thermodynamic conditions are

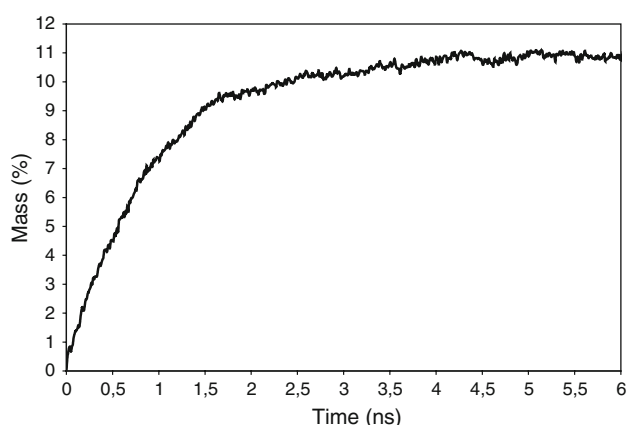


**Fig. 3** Results of the molecular dynamics modeling of the nanocapsule methane adsorption. Thermodynamic conditions are  $P = 40$  MPa and  $T = 300$  K

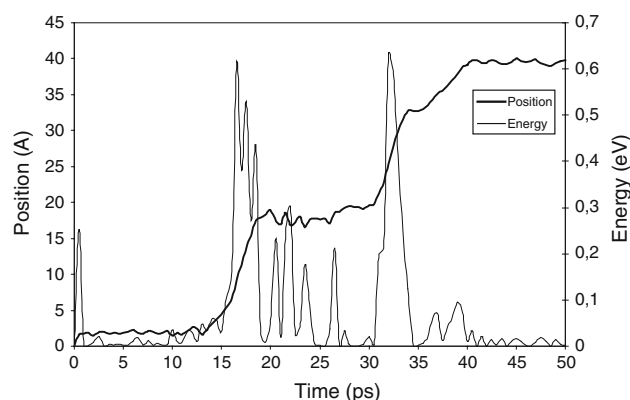


**Fig. 5** Results of molecular-dynamic modeling of the  $\text{K@C}_{60}^{1+}$  motion in the blocking chamber under the electric field action at the adsorption stage. The  $\text{K@C}_{60}^{1+}$  ion position with respect to the initial (time = 0 ps) ion position as a function of time. The change in the  $\text{K@C}_{60}^{1+}$  ion kinetic energy as a function of time

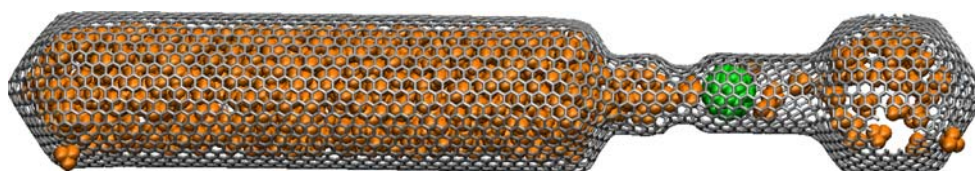


**Fig. 4** Nanocapsule closing stage ( $T = 300$  K,  $P = 40$  MPa)

brought to normal. The  $\text{K@C}_{60}^{1+}$ , which is located in the junction, moves to the blocking chamber under the methane pressure. However, its transfer is insignificant ( $\Delta d \sim 5 \text{ \AA}$ ) that is conditioned by the necessity to overcome the considerable energy barrier ( $\Delta E = 90 \text{ kcal/mol}$ ) to move to the blocking chamber. The nanocapsule state at the storage stage is shown in Fig. 6. The nanocapsule with methane molecules inside is in stable state. The calculations made show that there are no abnormal extensions of bonds between carbon atoms in the nanocapsule.

At the desorption stage when the temperature elevates from 300 K up to 350 K and the external pressure is normal, the  $\text{K@C}_{60}^{1+}$  endohedral complex in the junction is pushed into the blocking chamber under the expanding methane pressure, as shown in Fig. 7. Methane under pressure in the storage chamber freely desorbs into the external space through the holes in the blocking chamber. The availability of three holes in the blocking chamber and their configuration allow forcing out methane molecules and preserving the required rigidity of the construction. The holes are located in such a way that the  $\text{K@C}_{60}^{1+}$ , moving under the electric field action in the blocking chamber, is unable to block all its holes at once. The  $\text{K@C}_{60}^{1+}$  in the blocking chamber does not prevent methane desorption as the gas molecules flowing out do not touch it, and it is retained near the wall of the blocking chamber adjacent to the junction inlet—nanotube (10,10) due to the action of Van der Waals forces without the external electric field involved.

Figure 8 demonstrates the dependencies of the  $\text{K@C}_{60}^{1+}$  location stage and its kinetic energy upon time at the temperature elevation from  $T = 300 \text{ K}$  up to

$T = 350 \text{ K}$  at the stage of the  $\text{K@C}_{60}^{1+}$  desorption into the blocking chamber. At 3 ps, the significant increase in the  $\text{K@C}_{60}^{1+}$  kinetic energy equaled to 2.05 eV (the  $\text{K@C}_{60}^{1+}$  velocity reaches 930 m/s) is observed. The  $\text{K@C}_{60}^{1+}$  kinetic energy is consumed for overcoming the considerable energy barrier ( $\Delta E = 90 \text{ kcal/mol}$ ) formed under the action of capillary forces. When the  $\text{K@C}_{60}^{1+}$  passes the energy barrier, the kinetic energy decreases considerably to 0.41 eV ( $t = 5 \text{ ps}$ ). After passing the junction at 7 ps the  $\text{K@C}_{60}^{1+}$  kinetic energy increases again and reaches 0.92 eV. When the  $\text{K@C}_{60}^{1+}$  gets into the blocking chamber, the oscillations between its walls are observed. Each zero value of the  $\text{K@C}_{60}^{1+}$  kinetic energy in the interval from 7 to 23 ps corresponds to the  $\text{K@C}_{60}^{1+}$  impact against the blocking chamber wall. Then, the insignificant impacts of the  $\text{K@C}_{60}^{1+}$  against the blocking chamber wall with further state stabilization near one of the pentagonal rings of the blocking chamber are observed (Fig. 7). The maximum kinetic energy is 2.05 eV, which is considerably smaller than the known value (200 eV) required for carbon nanotube destruction [22]. The maximum velocity of the  $\text{K@C}_{60}^{1+}$  motion is 930 m/s. The availability of even insignificant number of methane molecules in the blocking chamber considerably decreases the velocity of the  $\text{K@C}_{60}^{1+}$  motion, and, respectively, the kinetic energy of the  $\text{K@C}_{60}^{1+}$  impact against the blocking chamber wall.

The methane molecules desorption process is shown in Fig. 9. The thermodynamic conditions of desorption are very similar to the hyperbola function graph. The desorption stops at 25.4 ps, there are 53 methane molecules in the storage chamber, which is 1.38 mass%.

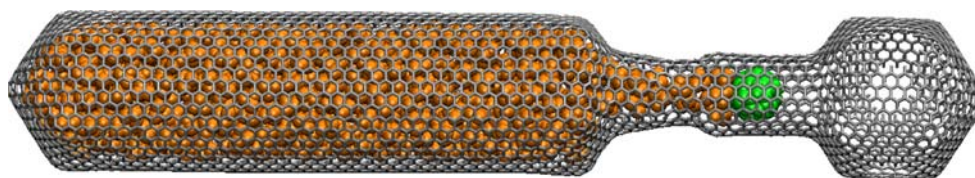


**Fig. 6** Methane storage stage ( $T = 300 \text{ K}$ ,  $P = 0.1 \text{ MPa}$ )



**Fig. 7** Methane desorption stage ( $T = 350 \text{ K}$ ,  $P = 0.1 \text{ MPa}$ )

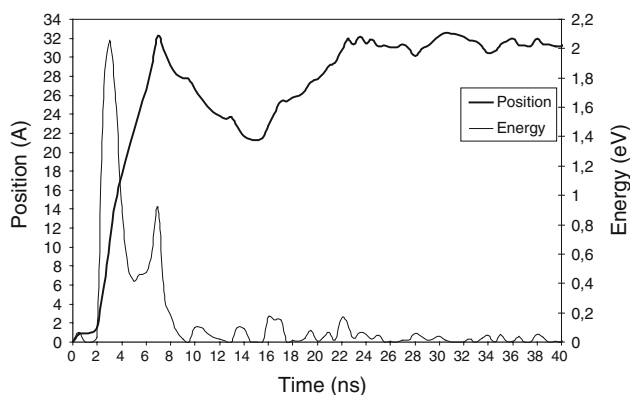


**Fig. 8** Results of molecular-dynamic modeling of the  $\text{K}@\text{C}_{60}^{1+}$  transfer at the temperature elevation up to 350 K.  $\text{K}@\text{C}_{60}^{1+}$  ion position with respect to the initial (time = 0 ps.) ion position as a function of time. The change in the  $\text{K}@\text{C}_{60}^{1+}$  ion kinetic energy as a function of time

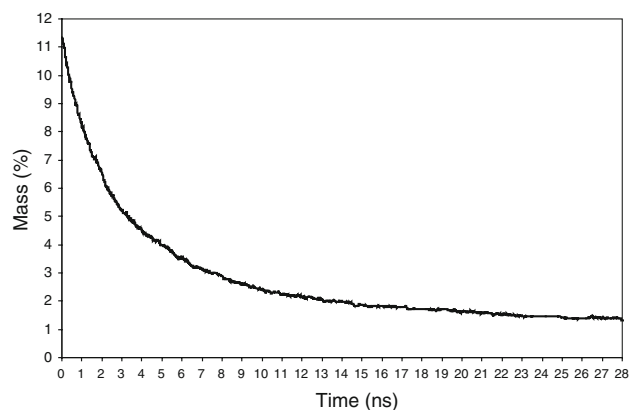


**Fig. 9** Results of the molecular dynamics simulation of methane molecules desorption from the nanocapsule. Thermodynamic conditions are  $P = 0.1$  MPa and  $T = 350$  K

## Conclusion

We demonstrated the functioning of the nanocapsule of complex structural shape for methane storage using the method of molecular dynamics. An obvious advantage of the nanocapsule is its operation cycle: methane is adsorbed under the elevated pressure (40 MPa) and at normal temperature with further blocking of methane molecules by the  $\text{K}@\text{C}_{60}^{1+}$  endohedral complex in the nanocapsule with the external electric field, the storage is performed in normal external conditions, and methane desorption is performed at temperature elevation up to 350 K, at which methane molecules push out the  $\text{K}@\text{C}_{60}^{1+}$  and are desorbed from the nanocapsule.

Methane content in the nanocapsule at the storage stage is  $\sim 11.09$  mass%. At the storage and desorption stages,

the electric field is not used, this significantly simplifies the use of nanocapsules in automobile applications.

The synthesis of similar nanocapsules is currently the task of experimenters. The multiple techniques of nanostructural engineering developed are the prerequisites for the creation of similar nanocapsules.

**Acknowledgments** Calculations are made in Interdepartmental Supercomputer Center of the Russian Academy of Science (Moscow).

## References

1. B.W. Smith, M. Monthieux, D.E. Luzzi, Encapsulated C60 in carbon nanotubes. *Nature* **396**, 323–324 (1998)
2. B.W. Smith, D.E. Luzzi, Formation mechanism of fullerene peapods and coaxial tubes: a path to large scale synthesis. *Chem. Phys. Lett.* **321**, 169–174 (2000)
3. H.W. Kroto, J.R. Heath, S.C. O'Brien, R.F. Curl, R.E. Smalley, C60: buckminsterfullerene. *Nature* **318**(6042), 162–163 (1985)
4. S. Iijima, Helical microtubules of graphitic carbon. *Nature* **354**(6348), 56–58 (1991)
5. Y.-K. Kwon, D. Tomanek, S. Iijima, “Bucky Shuttle” memory device: approach and molecular dynamic simulations. *Phys. Rev. Lett.* **82**, 1470–1473 (1999)
6. D. Baowan, N. Thamwattana, J. Hill, Encapsulation of C60 fullerenes into single-walled carbon nanotubes: Fundamental mechanical principles and conventional applied mathematical modeling. *Phys. Rev. B* **76**, 155411–155418 (2007)
7. Y.X. Ren, T.Y. Ng, K.M. Liew, State of hydrogen molecules confined in C60 fullerene and carbon nanocapsule structures. *Carbon* **44**(3), 397–406 (2006)
8. X. Ye, X. Gu, X.G. Gong, T.K.M. Shing, Z.F. Liu, A nanocontainer for the storage of hydrogen. *Carbon* **45**(2), 315–320 (2007)
9. R.E. Barayas-Barraza, R.A. Guirado-Lopez, Clustering of H<sub>2</sub> molecules encapsulated in fullerene structures. *Phys. Rev. B Condens. Matter* **66**(15), 155426.1–155426.12 (2002)
10. T. Oku, M. Kuno, Synthesis, argon/hydrogen storage and magnetic properties of boron nitride nanotubes and nanocapsules. *Diamond Relat Mater* **12**(3–7), 840–845 (2003)
11. A.V. Vakhrushev, M.V. Suyetin, Methane storage in bottle-like nanocapsules. *Nanotechnology* **20**, 125602.1–125602.5 (2009)
12. M.V. Suyetin, A.V. Vakhrushev, Nanocapsule for safe and effective methane storage. *Nanoscale Res. Lett.* (2009). doi: [10.1007/s11671-009-9391-x](https://doi.org/10.1007/s11671-009-9391-x)
13. M.V. Suyetin, A.V. Vakhrushev, Temperature sensitive nanocapsules for methane storage. *Micro Nano Lett.* (2009). (Accepted)
14. A.V. Krashennnikov, F. Banhart, Engineering of nanostructured carbon materials with electron or ion beams. *Nat. mater.* **9**, 723–733 (2007)
15. F. Banhart, J.X. Li, A.V. Krashennnikov, Carbon nanotubes under electron irradiation: stability of the tubes and their action as pipe for atom transport. *Phys. Rev. B* **71**(24), 241408.1–241408.4 (2008)
16. F. Banhart, Irradiation of carbon nanotubes with focused electron beam in the electron microscope. *J. Mater. Sci.* **41**, 4505–4511 (2006)
17. J.C. Phillips, R. Braun, W. Wang, J. Gumbart, E. Tajkhorshid, E. Villa et al., Scalable molecular dynamics with NAMD. *Comp. Chem.* **26**, 1781–1802 (2005)
18. W. Humphrey, A. Dalke, K. Schulten, VMD—visual molecular dynamics. *J. Molec. Graphics* **14.1**, 33–38 (1996)

19. A.D. Becke, A new mixing of Hartree–Fock and local density functional theories. *J. Chem. Phys.* **98**(2), 1372–1377 (1993)
20. A.D. Becke, Density—functional thermochemistry I. The effect of the exchange—only gradient correction. *J. Chem. Phys.* **96**(3), 2155–2160 (1992)
21. M.J. Frisch, G.W. Trucks, H.B. Schlegel, G.E. Scuseria, M.A. Robb, J.R. Cheeseman, et al., *Gaussian 98 (Revision A.1)*. (US. Gaussian Inc, Pittsburgh, PA, 1998)
22. H.-G. Busmann, Th. Lill, I.V. Hertel, Near specular reflection of C60 ions in collisions with an HOPG graphite surface. *Chem. Phys. Lett.* **187**(5), 459–465 (1991)